Current stress state and principal stress rotations in the vicinity of the Chelungpu fault induced by the 1999 Chi-Chi, Taiwan, earthquake

Weiren Lin,[1] En-Chao Yeh,[2] Hisao Ito,[3] Jih-Hao Hung,[4] Tetsuro Hirono,[5] Wonn Soh,[1] Kuo-Fong Ma,[4] Masataka Kinoshita,[6] Chien-Ying Wang,[4] and Sheng-Rong Song[2]

Received 3 May 2007; revised 10 July 2007; accepted 24 July 2007; published 23 August 2007.

[1] We carried out various stress measurements in boreholes penetrating the northern segment of the Chelungpu fault, drilled about 5 years after the 1999 Chi-Chi, Taiwan, earthquake. In the possible depth range of the Chelungpu fault, three major fault zones were encountered. Clearly recognizable principal stress rotations in the vicinity of the shallowest major fault zone, at 1133 m depth in hole B, suggest that this fault zone ruptured during the 1999 earthquake. Moreover, the fault's rupturing altered the stress state in the area surrounding this fault zone. In this paper, we constrain the possible magnitudes of the current principal horizontal stresses around the fault zone and show that the current stress state belongs to a normal or strike-slip fault regime. Therefore, the stress state was changed from that of a reverse fault regime by the rupturing.
Citation: Lin, W., E.-C. Yeh, H. Ito, J.-H. Hung, T. Hirono, W. Soh, K.-F. Ma, M. Kinoshita, C.-Y. Wang, and S.-R. Song (2007), Current stress state and principal stress rotations in the vicinity of the Chelungpu fault induced by the 1999 Chi-Chi, Taiwan, earthquake, *Geophys. Res. Lett.*, *34*, L16307, doi:10.1029/2007GL030515.

1. Introduction

[2] Stress and earthquakes are known to be interrelated: stress triggers earthquakes and earthquakes alter the shear and normal stresses on surrounding faults [*Stein*, 1999; *Hardebeck*, 2004; *Ma et al.*, 2005]. In this study, we focused on the second phenomenon, using an example from Taiwan. The huge, destructive Chi-Chi earthquake (Mw 7.6) occurred in west-central Taiwan in 1999 as a result of convergence of the Philippine Sea and Eurasian plates [*Kao and Angelier*, 2000; *Ji et al.*, 2003]. To understand the physics of the earthquake and the mechanism of rupture propagation, the Taiwan Chelungpu-fault Drilling Project (TCDP) drilled two vertical holes 40 m apart (hole A to an approximate depth of 2000 m and hole B to an approximate depth of 1350 m) about 2 km east of the surface rupture [*Ma et al.*, 2006]. The Chelungpu fault dips gently to the east (30°), and slips principally within and parallel to the bedding of the Pliocene Chinshui Shale. The TCDP holes penetrate three major fault zones [e.g., *Hirono et al.*, 2006] within the Chinshui Shale, which, despite its formal lithostratigraphic name, in this area is composed mainly of siltstone [*A. T. Lin et al.*, 2007].

[3] A main objective of the TCDP was to determine the spatial distribution of the in situ stress and, in particular, to determine the stress state on and around the fault plane before, during, and after the earthquake. Focal mechanisms of earthquakes occurring before the Chi-Chi earthquake [*Yeh et al.*, 1991], a stress tensor inversion of the Chi-Chi earthquake sequence [*Kao and Angelier*, 2001; *Wang and Chen*, 2001; *Ma et al.*, 2005; *Blenkinsop*, 2006], and a data set obtained from TCDP hole A [*Wu et al.*, 2007] provide some information about stress in the Taiwan area. However, we do not have sufficient satisfactory information about stress states obtained directly at depth near the Chelungpu fault. Therefore, we carried out a stress analysis, using both stress-induced compressive failures and drilling-induced tensile fractures, in TCDP hole B, and compiled the results along with several independent stress measurements based on the anelastic strain recovery (ASR) method and hydraulic fracturing tests. Importantly, the data suggest that the principal horizontal stress orientations rotated suddenly by about 90° in the vicinity of the Chelungpu fault induced by the 1999 Chi-Chi earthquake. Furthermore, we propose the possible magnitude range of the current principal horizontal stresses at depths around the fault zone that ruptured during this earthquake.

2. Orientations of Current Principal Horizontal Stress in TCDP Hole B

[4] We conducted downhole wireline logging with a Fullbore Formation MicroImager (FMI) to obtain electrical images of the borehole wall from about 930 to 1330 m depth in hole B. Three major fault zones were observed at depths of about 1133, 1191, and 1240 m, as determined by the wire length of the downhole logging tool. These depths usually are shallower by about 3 m from those determined from the drilling rod length. Since both stress-induced borehole breakouts and drilling-induced tensile fractures are dependent on in situ stress conditions, we can use information on their geometry, observed in the borehole wall images, to estimate orientations and magnitudes of in situ principal stresses in the plane perpendicular to the borehole axis [*Zoback et al.*, 1985, 2003; *Haimson*, 2007].

[5] We observed many breakouts and a few tensile fractures in the surveyed depth range in TCDP hole B.

[1]Kochi Institute for Core Sample Research, Japan Agency for Marine-Earth Science and Technology, Japan.
[2]Department of Geosciences, National Taiwan University, Taipei, Taiwan.
[3]Center for Deep Earth Exploration, Japan Agency for Marine-Earth Science and Technology, Yokohama, Japan.
[4]Institute of Geophysics, National Central University, Chung Li, Taiwan.
[5]Department of Earth and Space Science, Graduate School of Science, Osaka University, Osaka, Japan.
[6]Institute for Research on Earth Evolution, Japan Agency for Marine-Earth Science and Technology, Yokosuka, Japan.

0094-8276/07/2007GL030515$05.00

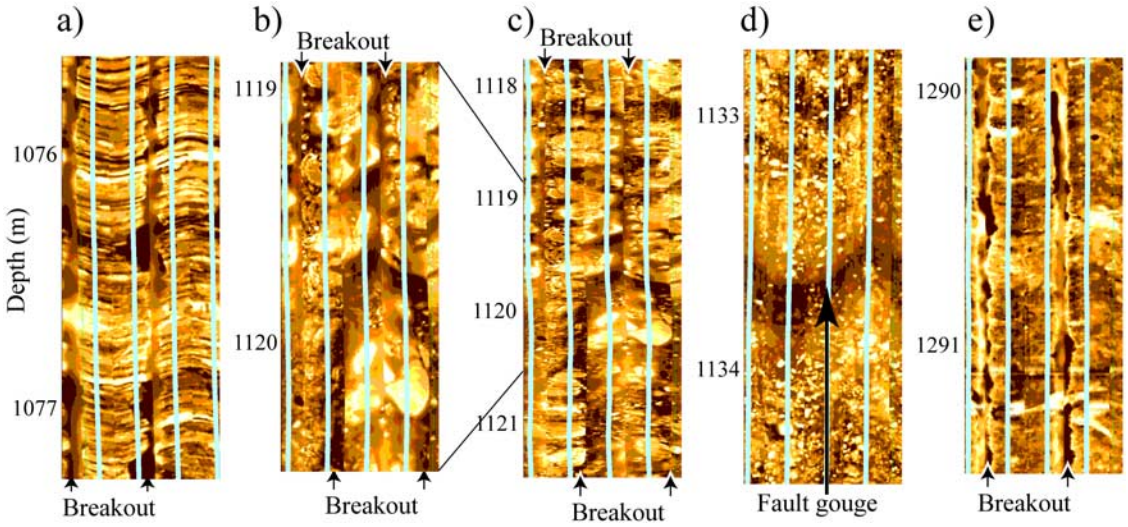

Figure 1. Unrolled electrical images of borehole walls at four depths in TCDP hole B. Dark color in the images represent conductive and light color resistive areas. (a) Breakouts at around 1076 m depth, above the shallowest major fault zone (FZ); (b, c) breakouts showing sudden rotation of the orientations of the horizontal principal stress at around 1120 m on different scales; (d) image from the center of the shallowest FZ; and (e) breakouts at about 1290 m depth, below the FZ.

Figures 1a, 1b, 1c, and 1e show breakouts at depths far above, immediately above, and far beneath the shallowest major fault zone, respectively. Breakouts or tensile fractures, if present, are always found in pairs, with one member of the pair opposite the other in the borehole wall, as shown in Figure 1. In addition, the difference in orientation between the two positions is always about 180°. We recorded the azimuth data of breakouts and tensile fractures according to following criteria, and plotted the azimuth distribution of the maximum principal horizontal stress $S_{H\max}$ (Figure 2). The criteria used were (1) breakouts are wider than a fracture and do not have sharp, straight boundaries like a tensile fracture does, (2) breakouts or tensile fractures must occur in pairs and in two opposite positions, that is, not on only one side of the borehole wall, and (3) breakouts or tensile fractures are equal to or longer than approximately 0.5 m. Because we conducted the FMI logging in hole B about 5 years and 7 months after the last slip event, the results represent the current, post-seismic stress state.

[6] The $S_{H\max}$ azimuths were mostly distributed between 105° and 155° at all surveyed depths, except at around 1133 m. The average azimuths were concentrated within the relatively narrow range from 119° (near 1170 m depth) to 133° (near 1300 m). This azimuth of N119–133°E is consistent with the downdip direction of the bedding planes of the Chinshui Shale, and is also the same as the azimuth of rupture of the Chelungpu fault during the 1999 Chi-Chi earthquake [*A. T. Lin et al.*, 2007]. This orientation is in good agreement with the regional stress state at the TCDP drilling site obtained from fault slip analyses of the Chi-Chi earthquake data [*Kao and Angelier*, 2001; *Blenkinsop*, 2006] and tectonic stress data for central Taiwan [*Yeh et al.*, 1991].

[7] In a narrow depth interval at around 1133 m depth, the $S_{H\max}$ azimuth (212° on average) importantly differs by about 90° from the azimuths at other depths. Moreover, the $S_{H\max}$ azimuth at about 1133 m in hole B is consistent with the stress orientation estimated by the ASR method at the depth of the shallowest major fault zone in hole A [*W. Lin et al.*, 2007]. In the electrical image from immediately above (1120 m depth) the shallowest major fault zone (Figures 1b and 1c), the azimuth of the breakouts is suddenly rotated by about 90°; in other words, at this depth, the orientation of $S_{H\max}$ changes roughly from an azimuth parallel to the fault rupture direction to one perpendicular to the direction of rupture. Similarly, in the SAFOD pilot hole, *Hickman and Zoback* [2004] observed drastic rotation of the localized principal stress orientation around fault zones; for example, the apparent azimuth of $S_{H\max}$ just below a minor fault gradually changed by about 70° over an interval of only 5 m. In addition, *Yamashita et al.* [2004] reported that the Nojima fault slip of the 1995 Kobe earthquake induced rotation of the principal stress axis orientation. Moreover, *Barton and Zoback* [1994] presented additional examples of stress rotation associated with fault movements. However, the stress change observed in this study differs from those mentioned by these previous studies in that maximum principal horizontal stress, $S_{H\max}$, and the minimum principal horizontal stress, $S_{h\min}$, can be considered to have been interchanged in the vicinity of the fault. This difference probably relates to the difference in fault movements: the Chelungpu fault is a thrust fault, whereas the Nojima fault is a strike-slip fault.

[8] Even though some scientists believe that the shallowest major fault zone (1133 m) is the one that ruptured during the 1999 Chi-Chi earthquake [e.g., *Wu et al.*, 2007], additional data verifying which fault zone among the three major fault zones encountered by TCDP hole B slipped during the earthquake are still welcome. All three fault zones are in the Chinshui Shale, and all are within the possible depth range of the 1999 earthquake rupture, as indicated by abundant teleseismic data. *Kano et al.* [2006] and *Tanaka et al.* [2007] debate whether a temperature

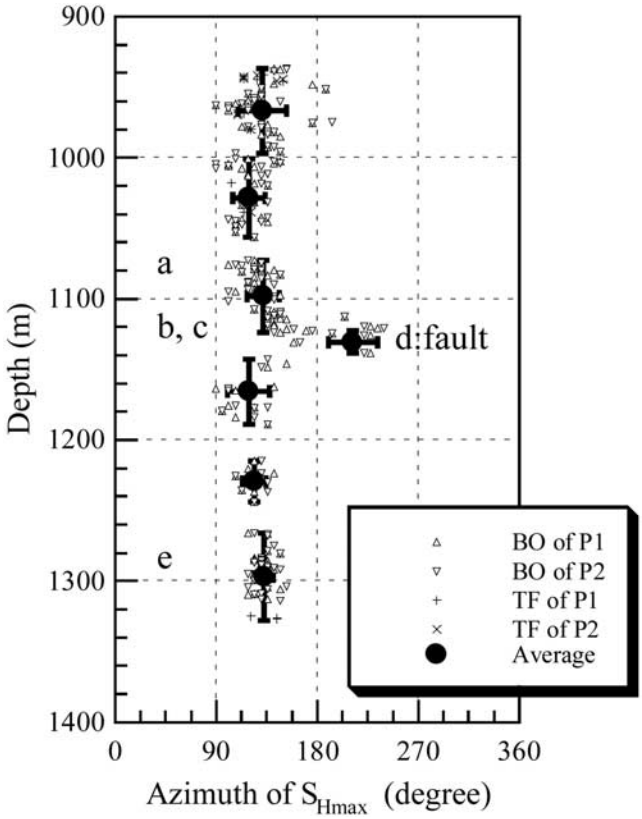

Figure 2. Azimuth distribution of the maximum principal horizontal stress S_{Hmax} determined from borehole breakouts ($\Delta\nabla$) and drilling-induced tensile fractures ($+\times$). Symbols $\Delta+$ and $\nabla\times$ refer to data obtained from the first or second running of the FMI logging, respectively. Letters a–e correspond to the respective locations of images in Figure 1, a–e. The solid circles show the average azimuths of $S_{H\max}$ from both breakouts and tensile fractures in each group; vertical bars show the depth range of the groups; horizontal error bars shows the standard deviations. Minimum and maximum azimuthal standard deviations of all groups were 9° and 22°, respectively. The accuracy of the azimuth data obtained from the borehole breakouts and the tensile fractures was generally approximately ±10–20°.

profile peak (positive thermal anomaly) around the shallowest major fault zone, determined by downhole measurement, was caused by frictional faulting associated with the 1999 earthquake. The stress orientation anomaly at around 1133 m depth, identified by this study, might constitute additional important evidence that the 1999 earthquake rupture occurred in the shallowest fault zone.

3. Constraints on Stress Magnitudes at Depths Near the Chelungpu Fault

[9] To constrain the magnitudes of $S_{H\max}$ and $S_{h\min}$ as well as that of the vertical stress S_v, we drew stress polygons in accordance with the Anderson theory of faulting [e.g., *Turcotte and Schubert*, 2002] and plotted our stress measurement results on the polygons (Figure 3). The three polygons were each composed of three triangles, representing the possible stress ranges of a reverse fault (RF), a strike-slip (SS), and a normal fault (NF) regime. The three polygons represent the possible ranges of principal horizontal stress magnitudes with coefficients of static friction μ = 1.0, 0.8, and 0.6, respectively, at 1120 m depth, where $S_{H\max}$ and $S_{h\min}$ were exchanged, based on the assumptions of a density-related lithostatic vertical-stress and a hydrostatic gradient pore-pressure. *Chen* [2005] conducted triaxial compressive tests under confining pressures of 20, 40, and 60 MPa on dry siltstone specimens with the same lithology as the rock at 1120 m depth and determined the coefficient of static friction of these specimens to be 0.8. Comparison of the possible stress ranges indicated by the three polygons for the three values of μ (Figure 3b) shows that the polygons do not differ very much in the lower stress area where the in-situ stress are obtained, but for the RF regime, the top boundaries of the polygons differ significantly among the three cases.

[10] In addition, the red lines, labeled BO for breakout in Figure 3, show the stress magnitude limits allowing breakout development, based on a minimum value of 32.9 MPa for the uniaxial compressive strength *Sc* of the siltstone, determined under water-saturated conditions [*Chen*, 2005]. We estimated the stress condition limits using the method of *Moos and Zoback* [1990] and adopted the uniaxial compressive strength as the failure criterion for breakout development, although *Moos and Zoback* [1990] mentioned that the strength should be equal to or larger than the uniaxial compressive strength and equal to or less than the biaxial compressive strength. It is clear that the criterion we adopted might result in a lower stress magnitude limit for breakout appearance. Thus, the stress state at the depth of 1120 m should be in the area above and to the left of the two red lines and within the polygons. On the other hand, the stress state limit allowing formation of drilling-induced tensile fractures was determined on the basis of a rock tensile strength *St* = 0, because of possible preexisting fractures and cracks, and is shown by the green line labeled DITF. Because tensile fractures are absent at 1040–1300 m depth, which is roughly the depth range of the Chinshui Shale, the possible stress state in that depth range should be in the area to the right of the green line and within the polygons. Considering both limits, the stress state at around 1120 m depth should be in the area between the red and green lines and within the polygons.

[11] *Barton et al.* [1988] proposed a simple method for estimating the magnitude of $S_{H\max}$ using $S_{h\min}$, the width of the breakouts, and the uniaxial compressive strength of the rock. Although this simple method has since been improved [e.g., *Vernik and Zoback*, 1992; *Haimson and Chang*, 2002], we used the simple method of *Barton et al.* [1988] because we did not have true triaxial compression test data as required by the improved methods, and the simple method has been successfully used in a number of deep scientific drill holes [*Zoback et al.*, 2003]. We estimated $S_{H\max}$ by using the several values for $S_{h\min}$ obtained by hydraulic fracturing tests, the width of the breakouts at around 1120 m depth, and minimum and maximum compressive strengths of 32.9 and 44.0 MPa, respectively [*Chen*, 2005]. We conducted hydraulic fracturing tests at four depths and obtained the minimum principal horizontal stress $S_{h\min}$ from the instantaneous shut-in pressure at those depths (J.-H. Hung et al., Structure geology, physical

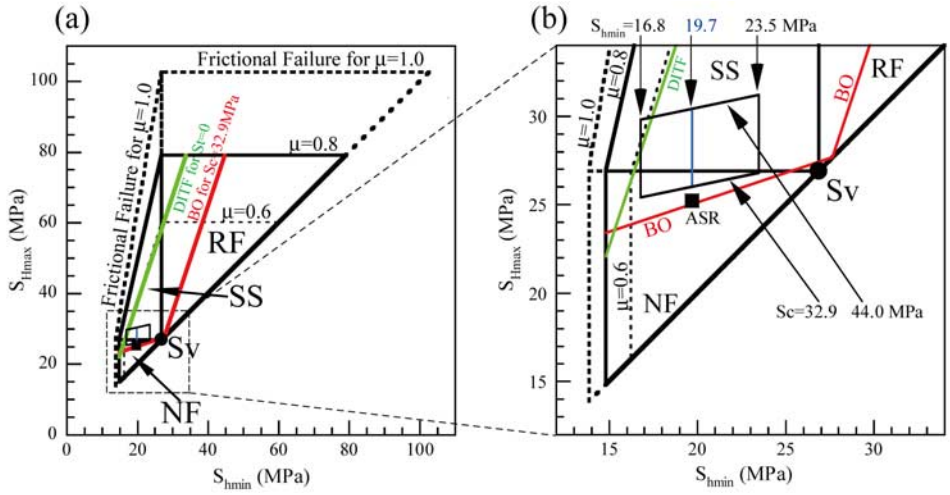

Figure 3. (a) Constraints on stress magnitude at 1120 m depth. (b) Expanded area corresponding to the square in Figure 3a. Stress polygons are based on the Anderson theory of faulting, with coefficients of static friction μ = 1.0, 0.8 and 0.6, respectively. The area enclosed by the red lines denoted by BO and green line by DITF is the possible stress distribution range given the observed presence of breakouts and the absence of tensile fractures at that depth for a compressive strength *Sc* = 32.9 MPa and tensile strength *St* = 0 MPa corresponding to the polygon of μ = 0.8. The parallelogram was plotted using two $S_{h\min}$ values from hydraulic fracturing test results at 1085 m and 1179 m depth, $S_{H\max}$ estimated from the breakout width, and measured maximum and minimum *Sc* values of siltstone from the Chinshui Shale. The blue line in the parallelogram shows the data based on the $S_{h\min}$ determined by ASR; the black square is the stress magnitudes based on the ASR test results.

property, fault zone characteristics and stress state in scientific drill holes of Taiwan Chelungpu Fault Drilling Project, submitted to *Tectonophysics*, 2007). We used only two values for $S_{h\min}$, 23.5 MPa and 16.8 MPa from 1085 m and 1179 m depth, respectively, because these depths are the nearest above and below the fault zone, respectively. Although the breakout width was not constant, the average width of 40° was approximately stable over several meters in the borehole. We show the ranges of $S_{h\min}$ and $S_{H\max}$ estimated from the different combinations of $S_{h\min}$ and S_c as a parallelogram (Figure 3b). The blue line in the parallelogram was estimated from the maximum and minimum S_c values and the $S_{h\min}$ value obtained by the ASR test [*W. Lin et al.*, 2007], and the solid square shows the $S_{h\min}$ and $S_{H\max}$ values calculated from the three-dimensional principal stress magnitudes estimated from the ASR test at 1112 m depth in hole A. The 1112 m depth of the ASR sample in hole A corresponds to the wireline depth of 1134 m in hole B. *W. Lin et al.* [2007] adopted ASR compliances calibrated from the overburden pressure value according to the method of *Lin et al.* [2006] to estimate the stress magnitudes from measured strain values obtained by ASR test.

[12] The stress magnitudes obtained by the ASR method, the hydraulic fracturing experiments, and the borehole breakout and tensile fracture analyses are consistent with one another. Moreover, the parallelogram may constrain the current stress state (postearthquake) around the northern segment of the Chelungpu-fault at about 1 km depth. The current stress state, 5–6 years after the Chi-Chi earthquake, is not within the reverse (or thrust) faulting regime, although reverse slip occurred on the fault plane during the earthquake. We believe that the current stress state reflects a stress-state change from RF to NF or SS caused by the fault's rupturing.

4. Conclusions

[13] Borehole breakout and tensile fracture data showed that the $S_{H\max}$ azimuth in most of the studied depth range (930–1330 m) coincided with the azimuth of the fault rupture, which was approximately the same as the downdip direction of the Chinshui Shale. However, the $S_{H\max}$ azimuth at around 1133 m depth, corresponding to the depth of the shallowest major fault zone, is at right angles to the azimuth of fault rupture, and the S_{hmin} azimuth coincides with the dip azimuth. This observation can be interpreted as a local interchange of the principal stresses. In addition, this stress orientation anomaly within a narrow depth interval around 1133 m might be important supporting evidence that this fault zone ruptured during the 1999 earthquake.

[14] We discussed the magnitudes of the horizontal principal stresses at 1120 m depth, immediately above the shallowest major fault zone on the basis of experimental hydraulic fracturing results, ASR measurements, breakout width, stress magnitude constraints in accordance with the Anderson theory of faulting, and experimental laboratory data. The stress magnitudes determined on the basis of the various measurements and theoretical analyses were in good agreement, and the results suggest that the current stress state at depths near the shallowest major fault zone is in a normal fault or strike-slip regime. The current stress state might reflect a stress-state change from RF before the earthquake to NF or SS after the earthquake as a result of the fault's rupturing.

[15] **Acknowledgments.** We gratefully acknowledge Y.-B. Tsai, one of the principal investigators of TCDP, Taiwan, and Y. Kawamura and T. Moe of CDEX/JAMSTEC, Japan, for giving us much helpful support for conducting the FMI logging in TCDP hole B. We also thank two anonymous reviewers for their constructive comments. A part of this work was supported by Grant-in-Aid for Scientific Research (C: 19540453) of the JSPS, Japan.

References

Barton, C. A., and M. D. Zoback (1994), Stress perturbations associated with active faults penetrated by boreholes: Possible evidence for near-complete stress drop and a new technique for stress magnitude measurement, *J. Geophys. Res.*, *99*, 9373–9390.

Barton, C. A., M. D. Zoback, and K. L. Burns (1988), In situ stress orientation and magnitudes at the Fenton geothermal site, New Mexico, determined from wellbore breakouts, *Geophys. Res. Lett.*, *15*, 467–470.

Blenkinsop, T. G. (2006), Kinematic and dynamic fault slip analyses: implications from the surface rupture of the 1999 Chi-Chi, Taiwan, earthquake, *J. Struct. Geol.*, *28*, 1040–1050.

Chen, C.-W. (2005), The study of the mechanical characteristics from the host rock of the Chelungpu Fault (in Chinese with English abstract), M.S., Thesis, 169 p, Natl. Taiwan Univ., Taipei.

Haimson, B. (2007), Micromechanisms of borehole instability leading to breakouts in rocks, *Int. J. Rock Mech. Min. Sci.*, *44*, 157–173.

Haimson, B. C., and C. Chang (2002), True triaxial strength of the KTB amphibolite under borehole wall conditions and its use to estimate the maximum horizontal in situ stress, *J. Geophys. Res.*, *107*(B10), 2257, doi:10.1029/2001JB000647.

Hardebeck, J. L. (2004), Stress triggering and earthquake probability estimates, *J. Geophys. Res.*, *109*, B04310, doi:10.1029/2003JB002437.

Hickman, S., and M. Zoback (2004), Stress orientations and magnitudes in the SAFOD pilot hole, *Geophys. Res. Lett.*, *31*, L15S12, doi:10.1029/2004GL020043.

Hirono, T., et al. (2006), High magnetic susceptibility of fault gouge within Taiwan Chelungpu fault: Nondestructive continuous measurements of physical and chemical properties in fault rocks recovered from Hole B, TCDP, *Geophys. Res. Lett.*, *33*, L15303, doi:10.1029/2006GL026133.

Ji, C., D. V. Helmberger, D. J. Wald, and K. Ma (2003), Slip history and dynamic implications of the 1999 Chi-Chi, Taiwan, earthquake, *J. Geophys. Res.*, *108*(B9), 2412, doi:10.1029/2002JB001764.

Kano, Y., J. Mori, R. Fujio, H. Ito, T. Yanagidani, S. Nakao, and K.-F. Ma (2006), Heat signature on the Chelungpu fault associated with the 1999 Chi-Chi, Taiwan earthquake, *Geophys. Res. Lett.*, *33*, L14306, doi:10.1029/2006GL026733.

Kao, H., and J. Angelier (2000), The Chi-Chi earthquake sequence: Active, out-of-sequence thrust faulting in Taiwan, *Science*, *288*, 2346–2349.

Kao, H., and J. Angelier (2001), Stress tensor inversion for the Chi-Chi earthquake sequence and its implications on regional collision, *Bull. Seismol. Soc. Am.*, *91*, 1028–1040.

Lin, A. T., S. M. Wang, J. H. Hung, M. S. Wu, and C. S. Liu (2007), Lithostratigraphy of the Taiwan Chelungpu-fault Drilling Project-A borehole and its neighboring region, central Taiwan, *Terr. Atmos. Oceanic Sci.*, *18*, 223–241, doi:10.3319/TAO.2007.18.2.223(TCDP).

Lin, W., M. Kwasniewski, T. Imamura, and K. Matsuki (2006), Determination of three-dimensional in-situ stresses from anelastic strain recovery measurement of cores at great depth, *Tectonophysics*, *426*, 221–238, doi:10.1016/j.tecto.2006.02.019.

Lin, W., et al. (2007), Preliminary results of stress measurement by using drill cores of TCDP hole-A: An application of anelastic strain recovery method to three-dimensional in-situ stress determination, *Terr. Atmos. Oceanic Sci.*, *18*, 379–393, doi:10.3319/TAO.2007.18.2.379(TCDP).

Ma, K.-F., C.-H. Chan, and R. S. Stein (2005), Response of seismicity to Coulomb stress triggers and shadows of the 1999 Mw = 7.6 Chi-Chi, Taiwan, earthquake, *J. Geophys. Res.*, *110*, B05S19, doi:10.1029/2004JB003389.

Ma, K.-F., et al. (2006), Slip zone and energetics of a large earthquake from the Taiwan Chelungpu-fault Drilling Project, *Nature*, *444*, 473–476, doi:10.1038/nature05253.

Moos, D., and M. D. Zoback (1990), Utilization of observations of well bore failure to constrain the orientation and magnitude of crustal stresses: Application to continental, Deep Sea Drilling Project, and Ocean Drilling Program boreholes, *J. Geophys Res.*, *95*(B6), 9305–9325.

Stein, R. S. (1999), The role of stress transfer in earthquake occurrence, *Nature*, *402*, 605–609.

Tanaka, H., W. M. Chen, K. Kawabata, and N. Urata (2007), Thermal properties across the Chelungpu fault zone and evaluations of positive thermal anomaly on the slip zones: Are these residuals of heat from faulting?, *Geophys. Res. Lett.*, *34*, L01309, doi:10.1029/2006GL028153.

Turcotte, D. L. and G. Schubert (2002), *Geodynamics*, 2nd ed., 456 pp., Cambridge Univ. Press, New York.

Vernik, L., and M. D. Zoback (1992), Estimation of maximum horizontal principal stress magnitude from stress-induced well bore breakouts in the Cajon Pass Scientific Research Borehole, *J. Geophys Res.*, *97*(B4), 5109–5119.

Wang, W.-H., and C.-H. Chen (2001), Static stress transferred by the 1999 Chi-Chi, Taiwan, earthquake: Effects on the stability of the surrounding fault systems and aftershock triggering with a 3D fault-slip model, *Bull. Seismol. Soc. Am.*, *91*, 1041–1052.

Wu, H.-Y., K.-F. Ma, M. Zoback, N. Boness, H. Ito, J.-H. Hung, and S. Hickman (2007), Stress orientations of Taiwan Chelungpu-Fault Drilling Project (TCDP) hole-A as observed from geophysical logs, *Geophys. Res. Lett.*, *34*, L01303, doi:10.1029/2006GL028050.

Yamashita, F., E. Fukuyama, and K. Omura (2004), Estimation of fault strength: Reconstruction of stress before the 1995 Kobe earthquake, *Science*, *306*, 261–263.

Yeh, Y.-H., E. Barrier, C.-H. Lin, and J. Angelier (1991), Stress tensor analysis in the Taiwan area from focal mechanisms of earthquakes, *Tectonophysics*, *200*, 267–280.

Zoback, M. D., D. Moos, L. Mastin, and R. N. Andersson (1985), Well bore breakouts and in-situ stress, *J. Geophys Res.*, *90*, 5523–5530.

Zoback, M. D., C. A. Barton, M. Brudy, D. A. Castillo, T. Finkbeiner, B. R. Grollimund, D. B. Moos, P. Peska, C. D. Ward, and D. J. Wiprut (2003), Determination of stress orientation and magnitude in deep wells, *Int. J. Rock Mech. Min. Sci.*, *40*, 1049–1076.

T. Hirono, Department of Earth and Space Science, Graduate School of Science, Osaka University, 1-1 Machikaneyama-cho, Toyonaka-shi, Osaka 560-0043 Japan.

J.-H. Hung, K.-F. Ma, and C.-Y. Wang, Institute of Geophysics, National Central University, 300 Jundga Road, Chung Li, 32001 Taiwan.

H. Ito, Center for Deep Earth Exploration, Japan Agency for Marine-Earth Science and Technology, 3173-25 Showa machi, Yokohama, Kanagawa, 236-0001 Japan.

M. Kinoshita, Institute for Research on Earth Evolution, Japan Agency for Marine-Earth Science and Technology, 2-15 Natsushima-cho, Yokosuka, Kanagawa, 237-0061 Japan.

W. Lin and W. Soh, Kochi Institute for Core Sample Research, Japan Agency for Marine-Earth Science and Technology, 200 Monobe-otsu, Nankoku, Kochi, 783-8502, Japan. (lin@jamstec.go.jp)

S.-R. Song and E.-C. Yeh, Department of Geosciences, National Taiwan University, P.O. Box 13-318, Taipei, 106 Taiwan.